EPJ Web of Conferences **3**, 04020 (2010)
DOI:10.1051/epjconf/20100304020

Few-nucleon contribution to π-scattering on light nuclei

S. Liebig[1,a], V. Baru[1], F. Ballout[1], C. Hanhart[1], and A. Nogga[1]

Institut für Kernphysik, Institute for Advance Simulation and Jülich Centre for Hadron Physics, Forschungszentrum Jülich, 52425 Jülich, Germany

Abstract. We present our new results of the few-nucleon contributions to π-^{2}H, π-^{3}He and π-^{4}He scattering lengths. To calculate these within the framework of Chiral Perturbation Theory we used a Monte-Carlo algorithm, which is briefly introduced. The size of the two-, three- and four-nucleon corrections in view of the expectations from two different power counting schemes is discussed. Based on our results, we estimate short range contributions, which limit the accuracy of the πN scattering lengths extracted from few-nucleon data. Additionally, we study how the π-^{4}He system constrains the determination of the isoscalar s-wave scattering length $a^{(+)}$ and its isovector counter part $a^{(-)}$.

1 Introduction

Assuming isospin symmetry, the πN scattering length can be decomposed in the following way

$$a_{\pi N} = \delta^{ab}\, a^{(+)} + i\epsilon^{abc}\tau^c\, a^{(-)}$$

into a part proportional to the isoscalar scattering length $a^{(+)}$ and a part proportional to its isovector counterpart $a^{(-)}$ (τ^i are the Pauli matrices for isospin, the indices a, b and c are isospin indices, and a sum over c is implied). Although these quantities are of fundamental interest, especially the isoscalar scattering length $a^{(+)}$ has not yet been determined experimentally with good accuracy, since it is very small compared to $a^{(-)}$. A more accurate determination of $a^{(+)}$ can only be successful when the few-nucleon contributions are well understood since the π-nucleus scatterin length can be written as [1]

$$a_{\pi A} = \left(\frac{1+\frac{m_\pi}{m_N}}{1+\frac{m_\pi}{A\,m_N}}\right)\left(A a^{(+)} - Q_\pi\, a^{(-)}\, 2T_3\right)$$

$$+ \text{ few-nucleon contributions}$$

$$+\text{isospin symmetry violating corrections}$$

where m_π and m_N are the pion and the nucleon mass, respectively, A the number of nucleons, Q_π the charge of the pion in units of e and T_3 the third component of the isospin of the nucleus. For isoscalar nuclei like ^{2}H and ^{4}He, T_3 equals zero, and the isoscalar scattering length $a^{(+)}$ could be extracted from a precise measurement of $a_{\pi A}$, if one were able to calculate the few-nucleon contributions in a controlled way (here we will not deal with isospin symmetry violating corrections which are studied in more detail in [2,3]). Therefore we study π-^{2}H, π-^{3}He and π-^{4}He scattering simultaneously to get a better understanding of the few-nucleon contributions and their systematics within the framework of Chiral Perturbation Theory (χPT).

Based on the symmetries of QCD one can formulate an effective field theory (EFT) formulated in terms of the relevant degrees of freedom. Considering the approximate chiral symmetry, which is spontaneously and explicitly broken giving rise to pseudo-Goldstone bosons (in this case the pions), the EFT in the low-energy domain is χPT, and the relevant degrees of freedom are pions and nucleons. χPT allows one to expand the effective Lagrangian $\mathcal{L}_{eff}$ in powers of $\frac{Q}{\Lambda_\chi}$, where Q is the pion mass m_π or a generic momentum, usually also assumed to be of order of the pion mass. However, in the literature it was argued that also the relatively small binding momentum could be a relevant scale. This proposal is investigated in Sec. 2. The chiral symmetry breaking scale Λ_χ is, for the specific process studied here, usually assumed to be of order of the ρ meson mass. With this expansion χPT provides a systematic scheme to identify a finite number of diagrams contributing to a given order, the so-called power counting.

2 π-nucleus scattering

Applying this power counting naively to the pion-scattering process the one-nucleon contribution (Fig. 1) is identified to be the leading one, proportional to m_π/f_π^2, where $f_\pi = 92.4\,\text{MeV}$ is the pion decay constant. However, this diagram will not contribute to π-^{2}H and π-^{4}He scattering because of its isospin structure. Nevertheless we are going

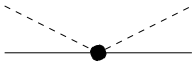

Fig. 1. Feynman diagram for the leading one-nucleon contribution to π-nucleus scattering. Solid lines denote nucleons, dashed lines pions.

[a] e-mail: s.liebig@fz-juelich.de

to use this order of magnitude estimate to analyse the suppression of the two-nucleon contributions shown in Fig. 2.

The following diagrams contribute to π-^{2}H scattering to $O\left(Q^3\right)$:

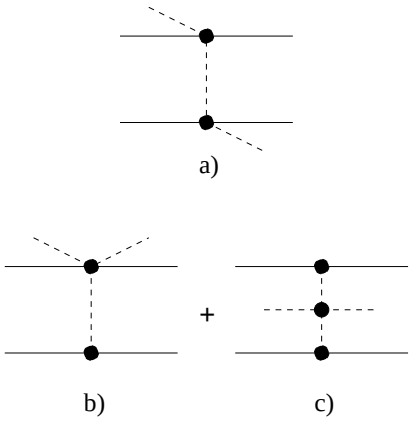

Fig. 2. Coulombian (diagram a)) and non-Coulombian (diagrams b)+c)) two-nucleon contributions to π-nucleus scattering

With the Feynman rules derived from the effective chiral Lagrangian, the explicit expressions for the two-nucleon operators associated with diagram 2a) and diagrams 2b) + 2c), respectively, read [4,5]:

$$iM^{(2a)} = i\frac{m_\pi^2}{4f_\pi^4\,\mathbf{q}^2}\left\{2\delta^{ab}\,(\boldsymbol{\tau}_1\cdot\boldsymbol{\tau}_2) - \tau_1^b\tau_2^a - \tau_1^a\tau_2^b\right\} \quad (1)$$

$$iM^{(2bc)} = -i\frac{g_A^2 m_\pi^2}{4f_\pi^4}\frac{1}{\left(\mathbf{q}^2+m_\pi^2\right)^2}\,(\boldsymbol{\sigma}_1\cdot\mathbf{q})\,(\boldsymbol{\sigma}_2\cdot\mathbf{q}) \times\left\{\delta^{ab}\,(\boldsymbol{\tau}_1\cdot\boldsymbol{\tau}_2) - \left(\tau_1^a\tau_2^b+\tau_1^b\tau_2^a\right)\right\}, \quad (2)$$

where g_A is the axial-vector coupling constant, $\boldsymbol{\sigma}_i$ the Pauli matrices for spin of the i-th nucleon and $\mathbf{q}$ the momentum transfer between the nucleons. Naive dimensional analysis reveals that diagram 2a) is proportional to $\left(m_\pi^2\,\mathbf{q}\right)/\left(f_\pi^2\,\Lambda_\chi^2\right)$ and thus acquires an additional factor of

$$\frac{m_\pi\,\mathbf{q}}{\Lambda_\chi^2}$$

relative to the one-nucleon contribution. Because of the structure of the denominator in Eq.(1) we are going to refer to the contribution of this diagram as the Coulombian contribution.
The two diagrams 2b) and 2c) need to be examined simultaneously since only their sum is independent of the choice of the pion-fields. They are suppressed by a factor of

$$\left(\frac{\mathbf{q}}{m_\pi}\right)^4$$

compared to the Coulombian two-nucleon contribution and will be referred to as the non-Coulombian contributions.

We want to study these relative scalings in view of two different power counting schemes:
Considering Weinberg's original power counting [4], where $|\mathbf{q}|$ is identified with m_π, both contributions are estimated to be of equal order of magnitude.

To account for the observed suppression of the non-Coulombian two-nucleon contributions, Beane et al. suggested a modified power counting, the so-called Q-counting [6], where $|\mathbf{q}|$ is assumed to be of order of the deuteron binding momentum γ. The deuteron binding momentum is related to the deuteron binding energy B_d via

$$\gamma = \sqrt{-B_\mathrm{d}\,m_N} \ll m_\pi\,. \quad (3)$$

In view of these two power counting schemes we analyse the few-nucleon contributions to π-^{3}He and π-^{4}He scattering in the following paragraph.
Fig. 3 shows the two classes of three-nucleon contributions that contribute to $O\left(Q^5\right)$ to π-^{3}He scattering. Explicitly, the operator from diagram 3a) reads:

$$iM^{(3a)} = \left(\frac{m_\pi}{2f_\pi^2}\right)^3\frac{1}{\mathbf{q}_1^2\,\mathbf{q}_3^2}\left\{\epsilon^{abe}\left[(\boldsymbol{\tau}_1\cdot\boldsymbol{\tau}_2)\,\tau_3^e + (\boldsymbol{\tau}_2\cdot\boldsymbol{\tau}_3)\,\tau_1^e\right]\right\}. \quad (4)$$

The $\mathbf{q}_i$ are the momentum transfers between the respective nucleon pairs, for details see [7]. Analogously to the two-nucleon case this contribution is going to be called Coulombian three-nucleon contribution.
For the second class of diagrams, where again only the sum of the diagrams 3b), 3c) and 3d) is independent of the choice of the pion-fields, the structure of the associated operators is very similar, so we only give an example here and refer to [7] for the full set of operators:

$$iM^{(3b)} = -\frac{g_A^2 m_\pi}{32f_\pi^6}\frac{1}{\left(\mathbf{q}_1^2+m_\pi^2\right)\left(\mathbf{q}_3^2+m_\pi^2\right)}\,(\boldsymbol{\sigma}_1\cdot\mathbf{q}_1)\,(\boldsymbol{\sigma}_3\cdot\mathbf{q}_3) \times\left\{\epsilon^{adf}\left(\tau_1^b\tau_3^d+\tau_1^d\tau_3^b\right)+\epsilon^{dbf}\left(\tau_1^a\tau_3^d+\tau_1^d\tau_3^a\right) +2\epsilon^{abf}\,(\boldsymbol{\tau}_1\cdot\boldsymbol{\tau}_3)\right\}\tau_2^f\,. \quad (5)$$

They are going to be named half-Coulombian.
Compared to the Coulombian two-nucleon contribution the Coulombian three-nucleon contribution scales as

$$\frac{m_\pi\,\mathbf{q}}{\Lambda_\chi^2}\,,$$

and, analogously to the two-nucleon case, we expect the half-Coulombian three-nucleon contributions to be suppressed by a factor of

$$\left(\frac{\mathbf{q}}{m_\pi}\right)^4$$

with respect to the Coulombian ones.
Three-nucleon contributions do not have to be considered

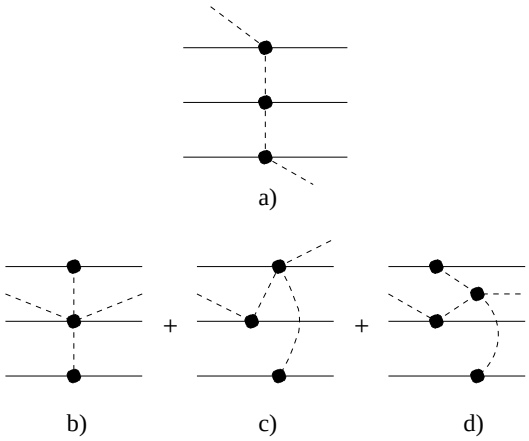

Fig. 3. Diagram a) shows the Feynman diagram for the Coulombian three-nucleon contribution. For the half-Coulombian three-nucleon contributions only the relevant topologies are depicted (diagrams b), c) and d)).

for π-^{4}He scattering since they are isovector. However, there are isoscalar four-nucleon contributions like the one depicted in Fig. 4. We expect this one to be the numerically most important four-nucleon contribution and consider it below to study the suppression of more-nucleon contributions.

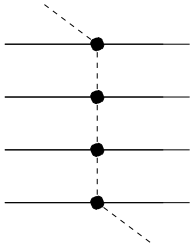

Fig. 4. Coulombian four-nucleon contribution to π-nucleus scattering

In the next paragraph we briefly introduce the numerical method that we used to evaluate the expectation values of the scattering operators.

3 Numerical method

The contribution of these diagrams to the π-nucleus scattering length can now be evaluated by calculating the expectation values of the pertinent expressions based on ^{2}H, ^{3}He and ^{4}He wave functions. We end up with a sum over all spin-isospin channels and integrals up to 18 dimensions (Fig.5):

$$\langle \hat{O} \rangle = \sum_{\alpha' \alpha} \int \frac{d^3p'_{12}}{(2\pi)^3} \frac{d^3p'_3}{(2\pi)^3} \frac{d^3q'_4}{(2\pi)^3} \int d^3p_{12}\, d^3p_3\, d^3q_4$$
$$\psi^*_{\alpha'} \left(\mathbf{p}'_{12}, \mathbf{p}'_3, \mathbf{q}'_4\right) \mathcal{M}_{\alpha' \alpha} \left(\mathbf{p}'_{12}, \mathbf{p}'_3, \mathbf{q}'_4, \mathbf{p}_{12}, \mathbf{p}_3, \mathbf{q}_4\right)$$
$$\psi_\alpha \left(\mathbf{p}_{12}, \mathbf{p}_3, \mathbf{q}_4\right), \quad (6)$$

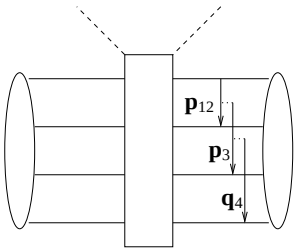

Fig. 5. Illustration of the few-nucleon contributions and the implied integrations over the Jacobi momenta $\mathbf{p}_{12}$, $\mathbf{p}_3$ and $\mathbf{q}_4$ in the 4N system.

where α and α' label the spin-isospin channel of in- and outgoing state, respectively. Note that for the wave functions, we normalised the momentum eigenstates to $\delta^{(3)}(\mathbf{p} - \mathbf{p}')$. Following common conventions, the operators are defined for a different normalisation, $\langle \mathbf{p}' | \mathbf{p} \rangle = (2\pi)^3 \delta^{(3)}(\mathbf{p} - \mathbf{p}')$. This is taken into account by the factors $\frac{1}{(2\pi)^3}$ as indicated in Eq.(6).

A convenient way to perform such high dimensional integrations is a Monte-Carlo method since the standard deviation does not depend on the dimensionality of the integral. The integral is evaluated by taking the average of the function values at random trial points that are in general uniformly distributed. To increase the efficiency we found it useful to also apply the so-called Metropolis algorithm [8] where a weight function is used to redistribute the trial points. For our purpose we chose this weight function according to the following conditions:

- The function needs to be maximal at the origin and drop to zero like some power r for large magnitudes of momenta.
- Its momentum dependence is largely caused by the magnitudes of the momenta and not by their directions.
- It needs to be positive, analytically integrable and normalised.

One possible choice is the ansatz

$$w\left(\mathbf{p}'_{12}, \mathbf{p}'_3, \mathbf{p}_{12}, \mathbf{p}_3\right) \equiv w\left(p'_{12}, p'_3, p_{12}, p_3\right)$$
$$= \prod_i \frac{(r-3)(r-2)(r-1)}{8\pi} \frac{C_{p_i}^{(r-3)}}{\left(p_i + C_{p_i}\right)^r}$$

for the weight function where the constants r and C_{p_i} were adjusted by minimizing the standard deviation in test cases. We checked the numerical reliability for the case of the deuteron, where we could also use standard techniques for the evaluation [7]. For ^{3}He and ^{4}He, the new technique enabled calculations in a very efficient way. The Metropolis algorithm was implemented in FORTRAN. Thereby the expressions of the operators for each spin-isospon channel could be added using Mathematica or Maple to generate the code lines based on the expressions given above. It turned out that the most CPU-time consuming part of the calculation was the generation of wave functions at arbitrary trial points for each spin-isospin channel.

4 Wave functions

We employed several wave functions for the numerical evaluation: phenomenological wave functions based on the CD Bonn [9] and AV18 [10] potentials, and wave functions based on chiral potentials. For these, we start with the leading one, given by the 1π-exchange and two contact interactions:

$$V(\mathbf{p}',\mathbf{p}) = -\left(\frac{g_A}{2f_\pi}\right)^2 \boldsymbol{\tau}_1\cdot\boldsymbol{\tau}_2\,\frac{\mathbf{q}\cdot\boldsymbol{\sigma}_1\,\mathbf{q}\cdot\boldsymbol{\sigma}_2}{\mathbf{q}^2+m_\pi^2} + C_S + C_T\,\boldsymbol{\sigma}_1\cdot\boldsymbol{\sigma}_2$$

The low-energy constants C_S and C_T parameterise the strength of the contact terms and are determined by a fit to NN scattering data and/or the deuteron.
In order to obtain a meaningful Schrödinger equation, it is necessary to introduce a regulator. We here perform regularisation by a smooth cutoff function given by

$$f(\mathbf{p}) = \exp\left(-\left(\frac{p}{\Lambda}\right)^4\right)$$

which depends on a cutoff parameter Λ. The potential is then replaced by

$$V(\mathbf{p}',\mathbf{p}) \longrightarrow f(\mathbf{p}')\,V(\mathbf{p}',\mathbf{p})\,f(\mathbf{p}).$$

To leading order (LO) the wave functions were given for a wide range of the cutoff parameter Λ (from 2 fm^{-1} to 20 fm^{-1}), and to next-to-leading (NLO) and to next-to-next-to-leading (N^{2}LO) order for five different pairs of the Lippmann-Schwinger cutoff Λ and the spectral function cutoff $\tilde{\Lambda}$ [11] between 2 and 3 fm^{-1}. We note here that three-nucleon forces do not contribute to LO and NLO to the chiral potentials which were used to generate the wave functions. This will be relevant for the discussion in Sec. 5. With the numerical results we test the relative scalings of the few-nucleon contributions estimated by the power counting schemes.

5 Results

For the π-^{2}H scattering process we came to the following results [7]:

With Weinberg's power counting scheme the two two-nucleon contributions (Fig. 2) are estimated to be of the same order of magnitude whereas Q-counting predicts a suppression of a factor of $(\mathbf{q}/m_\pi)^4$. With $|\mathbf{q}| \sim \gamma \approx \frac{1}{3}m_\pi$ (Eq.(3)) this factor is approximately $\frac{1}{100}$.
The numerical results are illustrated in Fig. 6. For the physical deuteron, the results support the suppression factor predicted by Q-counting. However, in addition the factor of $(\mathbf{q}/m_\pi)^4$ indicates a B_d^2-dependence of the non-Coulombian two-nucleon contributions (Fig.2bc) compared to the Coulombian ones (Fig. 2a) since $|\mathbf{q}| \propto \sqrt{B_\mathrm{d}}$. Studying an unphysical deuteron where the binding energy is varied between very small values like 0.001 MeV and very large values like 50 MeV by adjusting the parameters of the leading contact term in the deuteron channel we found that their ratio is not proportional to B_d^2. Therefore we restrict ourselves to Weinberg's power counting scheme to analyse the results for the three-nucleon contributions.

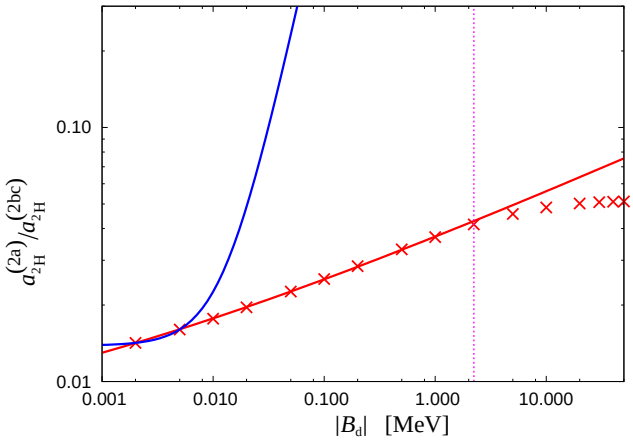

Fig. 6. Numerical results for the ratio of the non-Coulombian two-nucleon contributions with respect to the Coulombian ones. The red curve and crosses denote our results, the blue curve shows our expectation of a B_d^2-dependence and the pink dotted line marks the binding energy of the physical deuteron.

The two three-nucleon contributions (Fig. 3) are also estimated to be of equal order of magnitude, but the numerical results, given in Tab. 1, clearly show a suppression that turns out to be not parametric but due to spin-isospin factors.
Similar to the deuteron we examined the dependence of the π-^{3}He scattering lengths on the binding energy, illustrated in Fig. 7. As mentioned above the LO and NLO chiral potentials do not contain three-nucleon forces, therefore the binding energy of these wave functions still depends on the cutoff parameter.
The results for the Coulombian few-body contributions computed with the LO chiral wave functions reveal an almost linear dependence on the binding energy of ^{3}He analogous to the binding energy dependence of the *nd* scattering length known as Phillips line [12] showing the strong correlation of the two-nucleon contribution to the π-^{3}He scattering length.
Since the NLO and N^{2}LO chiral wave functions and the CD Bonn and AV18 wave functions reproduce the binding energy of ^{3}He satisfyingly the contribution to the scattering length in this order is much less cutoff dependent. Therefore, we want to restrict the subsequent discussion to the results of evaluations with these wave functions.

From naive dimensional analysis the relative suppression of the few-nucleon contributions relative to each other is expected to be

$$\frac{m_\pi\,\mathbf{q}}{\Lambda_\chi^2}\,.$$

Identifying $|\mathbf{q}|$ with m_π this gives

$$\left(\frac{m_\pi}{\Lambda_\chi}\right)^2 = \chi^2,$$

Table 1. Summary of the shifts of the scattering length due to the few-nucleon corrections $a_{^3\mathrm{He}}^{(2a)}$, $a_{^3\mathrm{He}}^{(2bc)}$, $a_{^3\mathrm{He}}^{(3a)}$, and $a_{^3\mathrm{He}}^{(3bcd)}$. For LO, the cutoff Λ is given in fm^{-1}, for NLO and N^{2}LO, both cutoffs ($\Lambda/\tilde{\Lambda}$) are given in MeV. Central values and standard deviation for the scattering length results are given.

	$\Lambda/\tilde{\Lambda}$	$a_{^3\mathrm{He}}^{(2a)}$ $\left[10^{-3}\, m_\pi^{-1}\right]$	$a_{^3\mathrm{He}}^{(2bc)}$ $\left[10^{-3}\, m_\pi^{-1}\right]$	$a_{^3\mathrm{He}}^{(3a)}$ $\left[10^{-3}\, m_\pi^{-1}\right]$	$a_{^3\mathrm{He}}^{(3bcd)}$ $\left[10^{-3}\, m_\pi^{-1}\right]$
CD Bonn	—	−25.081 ± 0.061	−0.329 ± 0.001	−4.02 ± 0.073	−0.789 ± 0.006
AV18	—	−24.127 ± 0.089	−0.884 ± 0.001	−3.536 ± 0.036	−0.728 ± 0.004
LO	2.0/ –	−30.203 ± 0.029	1.711 ± 0.001	−6.755 ± 0.123	−2.339 ± 0.006
LO	3.0/ –	−23.761 ± 0.129	−0.053 ± 0.001	−4.493 ± 0.038	−1.762 ± 0.004
LO	4.0/ –	−20.702 ± 0.252	−0.327 ± 0.001	−3.62 ± 0.025	−1.556 ± 0.015
LO	5.0/ –	−20.331 ± 0.129	−0.12 ± 0.001	−3.83 ± 0.093	−1.74 ± 0.015
LO	6.0/ –	−20.662 ± 0.104	0.099 ± 0.001	−3.941 ± 0.067	−1.96 ± 0.020
LO	8.0/ –	−21.452 ± 0.352	0.215 ± 0.002	−4.16 ± 0.149	−2.067 ± 0.021
LO	10.0/ –	−21.921 ± 0.992	0.128 ± 0.003	−4.283 ± 0.302	−1.872 ± 0.057
LO	12.0/ –	−19.554 ± 0.702	0.1 ± 0.005	−3.744 ± 0.391	−1.741 ± 0.015
LO	14.0/ –	−20.462 ± 0.869	0.167 ± 0.007	−3.364 ± 0.159	−1.652 ± 0.057
LO	16.0/ –	−18.935 ± 0.756	0.235 ± 0.010	−3.939 ± 0.701	−1.635 ± 0.043
LO	18.0/ –	−19.558 ± 0.987	0.295 ± 0.010	−4.359 ± 1.330	−1.712 ± 0.072
LO	20.0/ –	−19.22 ± 1.460	0.296 ± 0.018	−3.835 ± 0.894	−1.743 ± 0.158
NLO	400/500	−25.358 ± 0.040	0.828 ± 0.001	−3.934 ± 0.029	−0.695 ± 0.001
NLO	550/500	−24.326 ± 0.043	−0.061 ± 0.001	−3.431 ± 0.141	−0.374 ± 0.001
NLO	550/600	−24.047 ± 0.024	−0.037 ± 0.001	−3.245 ± 0.022	−0.397 ± 0.004
NLO	400/700	−25.234 ± 0.030	0.847 ± 0.001	−3.898 ± 0.021	−0.72 ± 0.002
NLO	550/700	−24.045 ± 0.054	−0.02 ± 0.001	−3.311 ± 0.015	−0.435 ± 0.004
N^{2}LO	450/500	−25.956 ± 1.069	0.642 ± 0.001	−3.979 ± 0.007	−0.721 ± 0.002
N^{2}LO	600/500	−25.602 ± 0.051	−0.021 ± 0.001	−3.826 ± 0.058	−0.496 ± 0.004
N^{2}LO	550/600	−25.55 ± 0.023	0.233 ± 0.001	−4.057 ± 0.075	−0.708 ± 0.004
N^{2}LO	450/700	−25.25 ± 0.039	0.611 ± 0.001	−4.038 ± 0.015	−0.806 ± 0.001
N^{2}LO	600/700	−25.51 ± 0.065	0.094 ± 0.001	−4.056 ± 0.053	−0.734 ± 0.002

for the ratio of the Coulombian two-nucleon (three-nucleon) contribution with respect to the leading one-nucleon (Coulombian two-nucleon) contribution to $a_{^3\mathrm{He}}$, and a suppression of χ^4 for the Coulombian four-nucleon contribution compared to the Coulombian two-nucleon contribution to $a_{^4\mathrm{He}}$. However, we observe a smaller suppression, for the π-^{3}He and the π-^{4}He scattering lengths listed in Table 2. One possible explanation for the observed deviation from the estimates is that naive dimensional analysis is not appropriate to estimate the relative scalings of the few-nucleon contributions with different numbers of nucleons relative to each other quantitatively. Also our estimate of the chiral symmetry breaking scale Λ_χ might be too large. Based on the cutoff parameters used for chiral interactions, Λ_χ = 500 MeV could be an equally justified choice. Concerning this issue further studies will be necessary. However, note that *n*-nucleon contributions among each other are well estimated within Weinberg's counting scheme.

6 Summary

Within the framework of χPT and with Weinberg's power counting scheme we identified the relevant few-nucleon contributions to π-scattering on light nuclei. We developed a Monte-Carlo algorithm of integration to evaluate their numerical contribution to the scattering lengths which enabled us to test the estimates of the power counting schemes. The contributing diagrams to π-^{4}He are summarised in Fig. 8, whereas Fig. 9 shows diagrams that turned out to be negligible.

Since the LO one-nucleon contribution (Fig. 1) does not contribute to π-scattering on isoscalar targets because of its isospin structure, higher order one-nucleon contributions need to be taken into account, the first one appearing at relative order χ^2. At the same relative order the Coulombian two-nucleon contribution contributes. Additionally, the leading isoscalar four-nucleon-two-pion contact term (diagram c) of Fig. 8) which is of relative order χ^4 needs to be considered. We estimate this short range contribution to the π-^{4}He scattering length to be $\sim 2 \cdot 10^{-3}\, m_\pi^{-1}$ which limits the accuracy of an extraction of $a^{(+)}$.
Another important diagram which has not been discussed in detail here is diagram 8d). Although it is of relative order χ^4 it is enhanced by a factor of π^2 which arises from singularities in the loop integration. For a further discussion and elaborate calculation we refer to [7].
On the other hand we found that we can neglect the non-Coulombian two-nucleon contributions (Fig. 9a)). As discussed above this sum of diagrams is not of relative order χ^2 but suppressed by spin-isospin factors. Diagram 9b) represents another class of diagrams that needs not to be taken into account. Such diagrams contribute at $\chi^{3/2}$ but

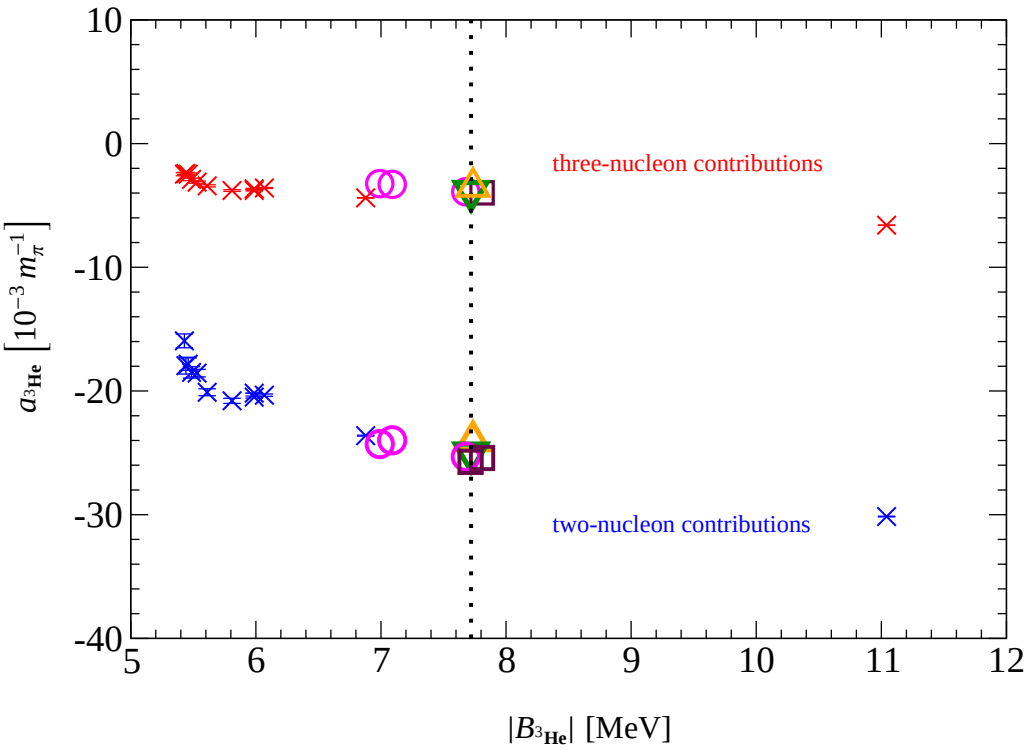

Fig. 7. $B_{^3\mathrm{He}}$-dependence of the Coulombian two- and three-nucleon contributions to π-^{3}He scattering. The results evaluated with the LO chiral wave functions are displayed by blue and red crosses for the two- and three-nucleon contributions, respectively. Circles: NLO, squares: N^{2}LO chiral wave functions, triangle down: CD Bonn, triangle up: AV18 wave function. The dotted line marks the binding energy of the physical ^{3}He. For the NLO (N^{2}LO) three (two) results were selected for each contribution since they are very close and therefore not distinguishable.

Table 2. Numerical results for the relative scalings of the few-nucleon contributions to π-^{3}He and π-^{4}He scattering compared to the estimates based on Weinberg–counting. For ^{4}He, we have not performed calculations for CD Bonn wave function.

	$\Lambda/\tilde{\Lambda}$	$a^{(2N)}_{^3\mathrm{He}}/a^{(1N)}_{^3\mathrm{He}}$	$a^{(3N)}_{^3\mathrm{He}}/a^{(2N)}_{^3\mathrm{He}}$	$a^{(2bc)}_{^3\mathrm{He}}/a^{(2a)}_{^3\mathrm{He}}$	$a^{(3bcd)}_{^3\mathrm{He}}/a^{(3a)}_{^3\mathrm{He}}$	$a^{(4N)}_{^4\mathrm{He}}/a^{(2N)}_{^4\mathrm{He}}$
CD-Bonn	—	0.276	0.189	0.013	0.196	—
AV18	—	0.272	0.170	0.037	0.206	0.054
NLO	400/500	0.267	0.189	0.033	0.177	0.053
NLO	550/500	0.265	0.156	0.003	0.109	0.043
NLO	550/600	0.262	0.151	0.002	0.122	0.040
NLO	400/700	0.265	0.189	0.034	0.185	0.076
NLO	550/700	0.262	0.156	0.001	0.131	0.050
N^{2}LO	450/500	0.275	0.186	0.025	0.181	0.060
N^{2}LO	600/500	0.279	0.169	0.001	0.130	0.087
N^{2}LO	550/600	0.275	0.188	0.009	0.175	0.045
N^{2}LO	450/700	0.268	0.197	0.024	0.200	0.047
N^{2}LO	600/700	0.276	0.188	0.004	0.181	0.054
Weinberg	—	0.040	0.040	1.000	1.000	0.002

turn out to cancel numerically (for details, see [13,14]). The Coulombian four-nucleon contribution is of relative order χ^6 and is therefore negligible.

Based on these insights we now have a controlled understanding of the few-nucleon contributions to π-scattering on light nuclei. However, for an accurate extraction of the isoscalar s-wave scattering length $a^{(+)}$ isospin symmetry violating corrections need to be included. This is in progress.

The work was supported in parts by funds provided from the Helmholtz Association (grants VH-NG-222, VH-VI-231), by the DFG (grants SFB/TR 16 and 436 RUS 113/991/0-1), by the EU HadronPhysics2 project. The work of V.B. was supported by the

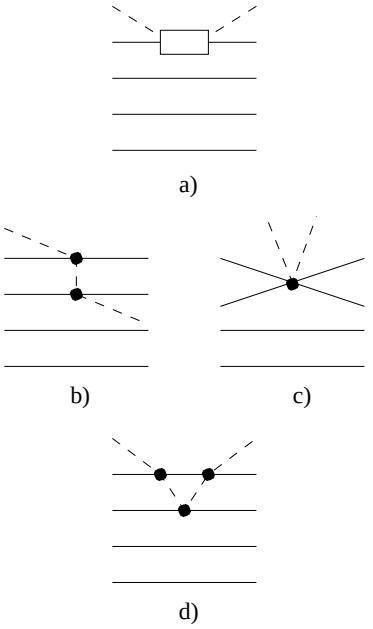

Fig. 8. Contributing diagrams to π-^{4}He scattering. Diagram a) shows the higher order one-nucleon contributions that first contribute at relative order χ^2, diagram b) the Coulombian two-nucleon contribution (relative order χ^2), diagram c) the leading isoscalar contact term (χ^4), and diagram d) which is enhanced by a factor of π^2.

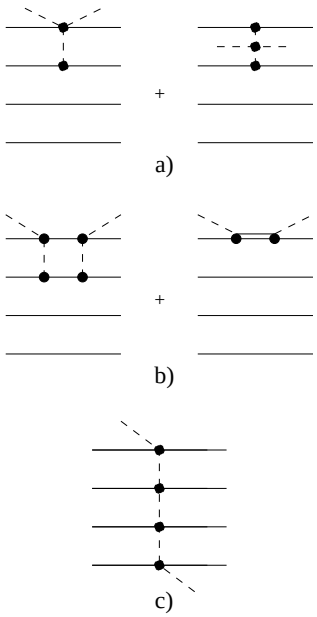

Fig. 9. Negligible contributions to π-^{4}He scattering. Diagram a) depicts the non-Coulombian two-nucleon contributions, diagram b) stands for a class of diagrams showing dispersive corrections and Δ-contributions that cancel numerically, and diagram c) shows the Coulombian four-nucleon contribution which is of relative order χ^6.

State Corporation of Russian Federation “Rosatom”.
The numerical calculations were performed on the supercomputer cluster of the JSC, Jülich.

References

1. V. Baru, J. Haidenbauer, C. Hanhart, and J. A. Niskanen, Eur. Phys. J. **A16** (2003) 437-446
2. J. Gasser, V. E. Lyubovitskij, and A. Rusetsky, Phys. Rept. **456** (2008) 167-251
3. Martin Hoferichter, Bastian Kubis, and Ulf-G. Meissner, Phys. Lett. **B678** (2009) 65-71
4. Steven Weinberg, Phys. Lett. **B295** (1992) 114-121
5. S. R. Beane, V. Bernard, T. S. H. Lee, and Ulf-G. Meißner, Phys. Rev. **C57** (1998) 424-426
6. S. R. Beane, V. Bernard, E. Epelbaum, Ulf-G. Meißner, and D. R. Phillips, Nucl. Phys. **A720** (2003) 399-415
7. S. Liebig, V. Baru, F. Ballout, C. Hanhart, and A. Nogga, in preparation.
8. N. Metropolis, A. W. Rosenbluth, M. N. Rosenbluth, A. H. Teller, and E. Teller , J. Chem. Phys. **21** (1953) 1087-1092
9. R. Machleidt, Phys. Rev. **C63** (2001) 024001
10. Robert B. Wiringa and V. G. J. Stoks and R. Schiavilla, Phys. Rev. **C51** (1995) 38-51
11. E. Epelbaum, W. Glöckle, and Ulf-G. Meißner, Nucl. Phys. **A747** (2005) 362-424
12. AC Phillips, Nucl.Phys. **A107** (1968) 209
13. V. Lensky, V. Baru, J. Haidenbauer, C. Hanhart, A. Kudryavtsev, and Ulf-G. Meißner, Phys. Lett. **B648** (2007) 46-53
14. V. Baru, J. Haidenbauer, C. Hanhart, A. Kudryavtsev, V. Lensky, and Ulf-G. Meißner, Phys. Lett. **B659** (2008) 184-191